


A practical primer on PI-RADS version 2: a pictorial essay

Gary Lloyd Horn Jr. ¹, Peter Florin Hahn,¹ Shahin Tabatabaei,² Mukesh Harisinghani¹

¹Division of Abdominal Imaging, Massachusetts General Hospital, White Building, Room 270, 55 Fruit Street, Boston, MA 02114, USA

²Department of Urology, Massachusetts General Hospital, 55 Fruit Street, Boston, MA 02114, USA

Abstract

Multiparametric magnetic resonance imaging has become an established method for evaluating the prostate for clinically significant prostate adenocarcinoma. Criteria have been developed for categorizing MRI findings, the most frequently used of which is the PI-RADS system. The PI-RADS V2 document provides separate image interpretation and clinical grading sections. Within this article we give an overview of the integrated, algorithmic way, we approach prostate MRI, show images corresponding to each PI-RADS category, and provide several illustrative cases.

Key words: Prostate—Magnetic resonance imaging—Prostatic neoplasms—PI-RADS

Multiparametric magnetic resonance imaging (mpMRI) has become an established technique for the detection and staging of clinically significant prostate adenocarcinoma. Recently, the American College of Radiology proposed and published the prostate imaging-reporting and data system (PI-RADS) V2 [1] as a synoptic reporting template for prostate cancer. Studies have since been completed validating the imaging parameters specified within this report [2], as well as mpMRI's role in active surveillance and targeting biopsies, increasing the diagnostic yield for clinically significant cancers [3–7]. This article aims to provide a simplified algorithm and imaging atlas to reference with the assessment and reporting portion of the PI-RADS V2 document.

PI-RADS V2 changes in comparison to V1

PI-RADS V2 recommends the use of high b value images (≥ 1400) for diffusion-weighted imaging (DWI) in the multiparametric analysis of prostate MRI images. Increasing b values has been shown to increase lesion conspicuity and identify clinically significant prostate cancers [8]. The main differences in image interpretation are as follow:

- The primary assessment of the peripheral and transition zones is now different, with the designation of a dominant sequence for each.
- The dominant sequences in evaluating the peripheral zone are high b value DWI and apparent diffusion coefficient (ADC).
- T2-weighted images are now used in the peripheral zone only to confirm the mass-like appearance of the observed restricted diffusion, to evaluate for extracapsular extension, and to give a PI-RADS score when DWI is inadequate (such as when there is artifact from a hip prosthesis).
- T2-weighted sequences are now dominant in the evaluation of the transition zone. Diffusion restriction now only plays a role in upgrading what would be a PI-RADS 3 lesion to a PI-RADS 4 lesion in the transition zone.
- Dynamic contrast enhancement (DCE) evaluation has been simplified. The absence or presence of enhancement before or at the same time as the rest of the prostate now differentiates lesions with minimal diffusion restriction into PI-RADS 3 and 4 lesions instead of the more complex washout curve analysis.
- MR spectroscopy is no longer a factor involved in PI-RADS scoring.
- New size criteria have been added. Lesions are differentiated based on size as measured on ADC for the peripheral zone and T2-weighted images for the

transition zone with lesions <1.5 cm being PI-RADS 4 and lesions ≥1.5 cm being PI-RADS 5. Other sequences can be used for measurement if the preferred dominant sequence is technically inadequate [1].

In the figures we provide an algorithmic approach to evaluate the prostate using the same method as PI-RADS V2 but in a simplified manner (Figs. 1, 2, 3). Additionally, images and illustrative cases are provided

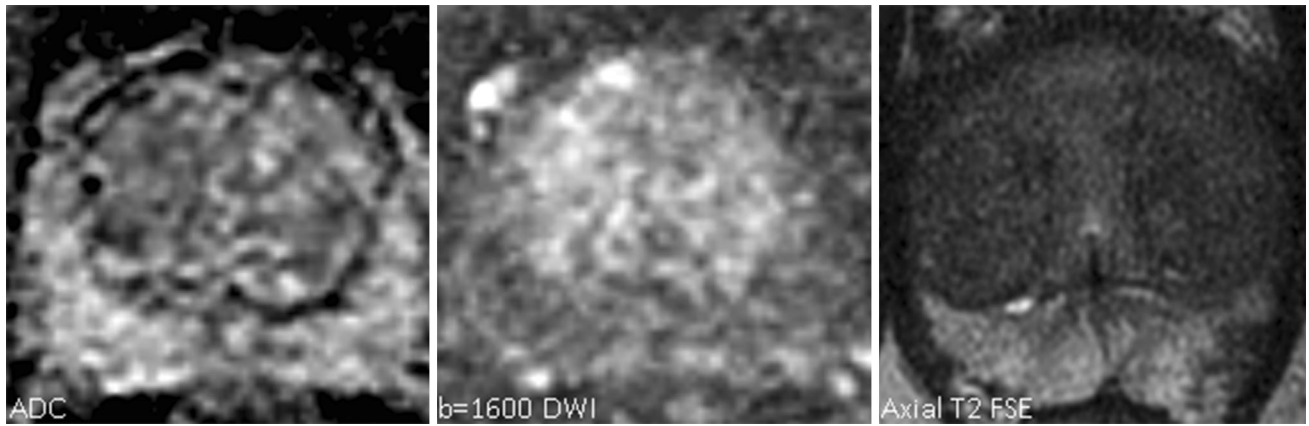


Fig. 1. PI-RADS 1 appearance of the peripheral zone on $b = 1600$ DWI/ADC (no abnormality) and the transition zone on T2 FSE (homogeneously intermediate signal intensity).

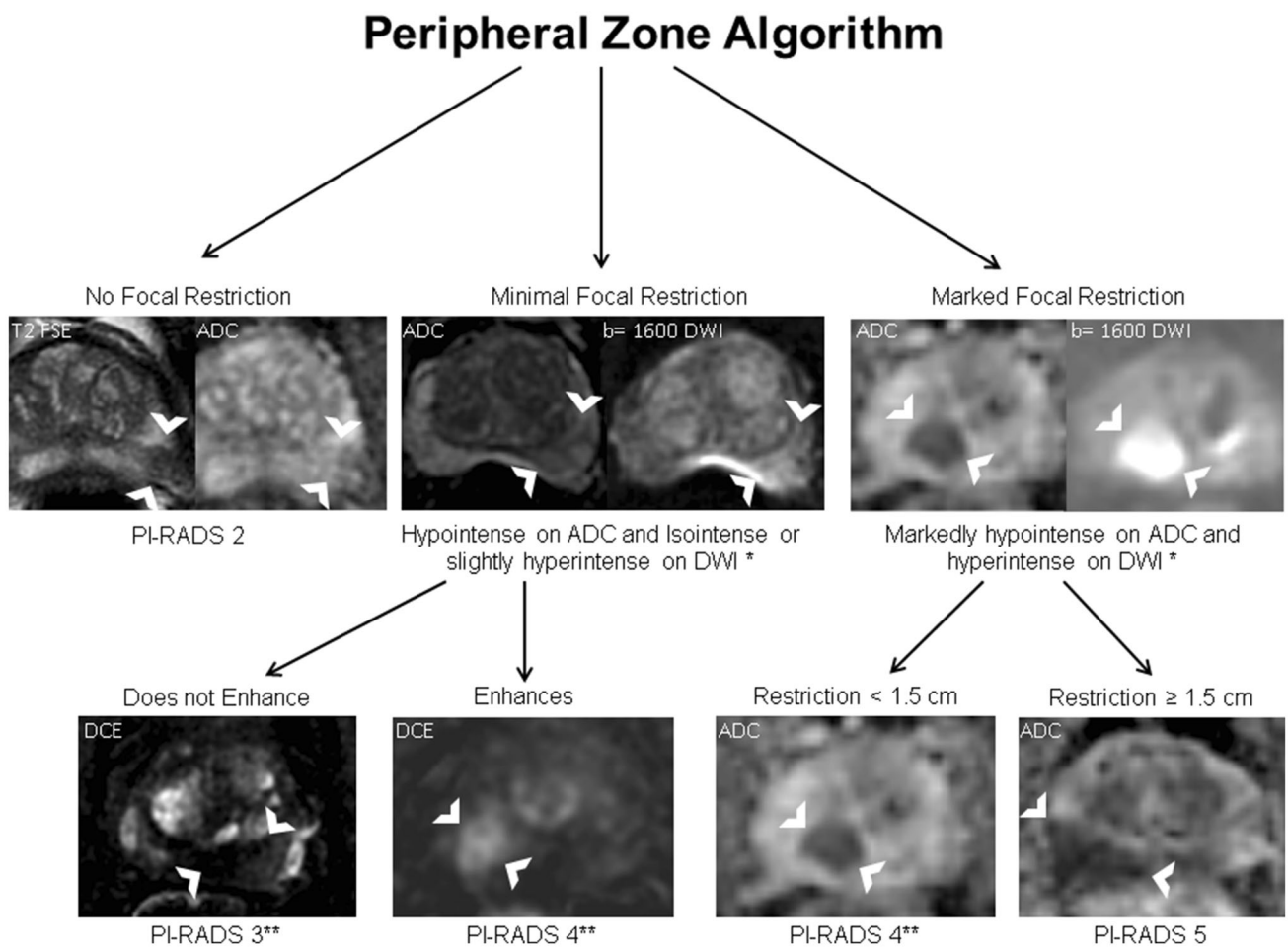


Fig. 2. An algorithm to follow for the evaluation of the peripheral zone. Denoted exceptions are as follow: *T1 signal within the prostate denotes hemorrhage from a prior biopsy

and makes evaluation of the affected area of the prostate unreliable (Fig. 4). **Any nodule with definite extraprostatic extension or invasive behavior is PI-RADS 5.

Transition Zone Algorithm

Focal T2 Abnormality

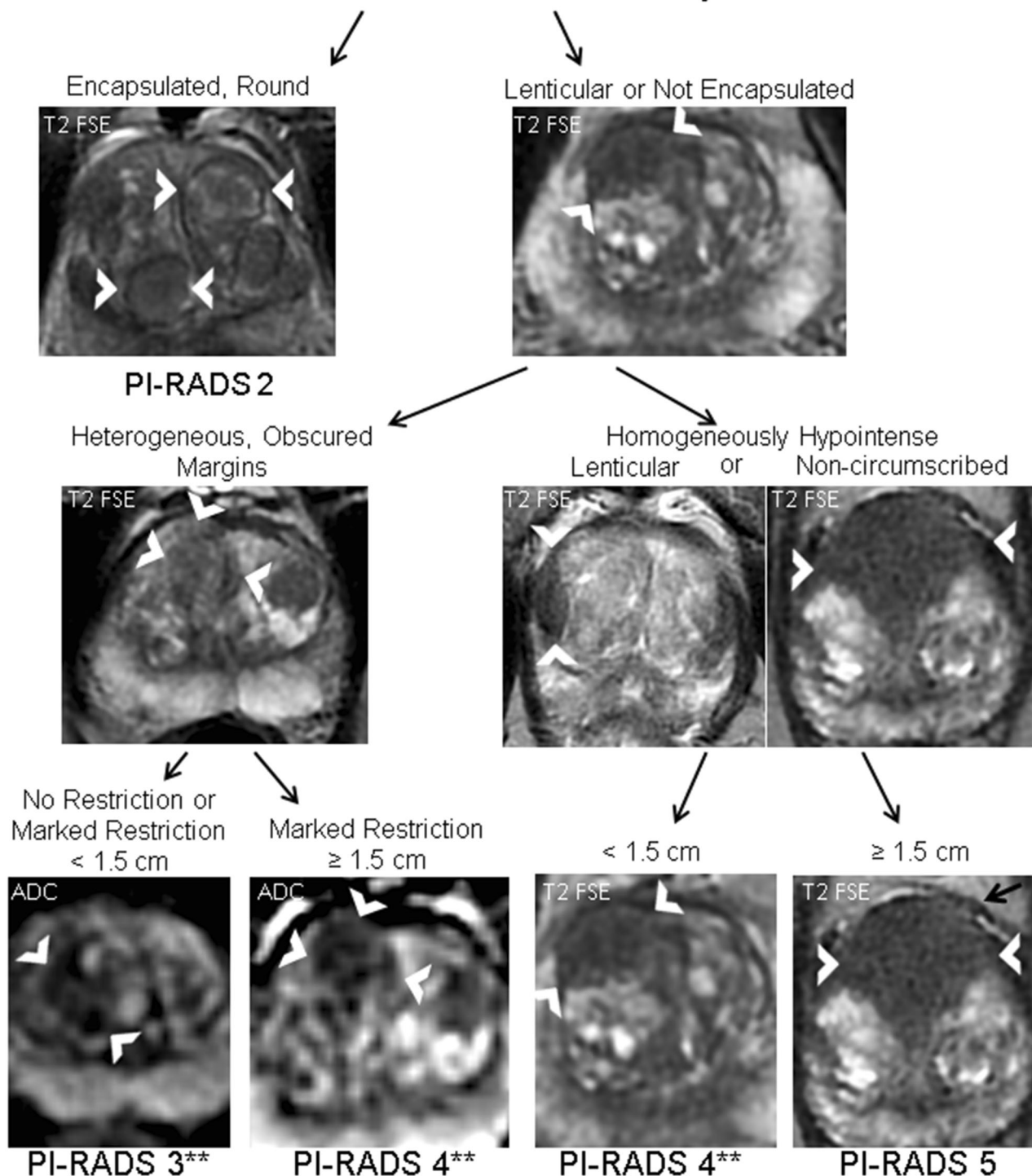


Fig. 3. An algorithm to follow for the evaluation of the transition zone. Denoted exception as follows: **Any nodule with definite extraprostatic extension or invasive behavior (seen in

the PI-RADS 5 lesion as denoted by the *black arrow*) is PI-RADS 5.

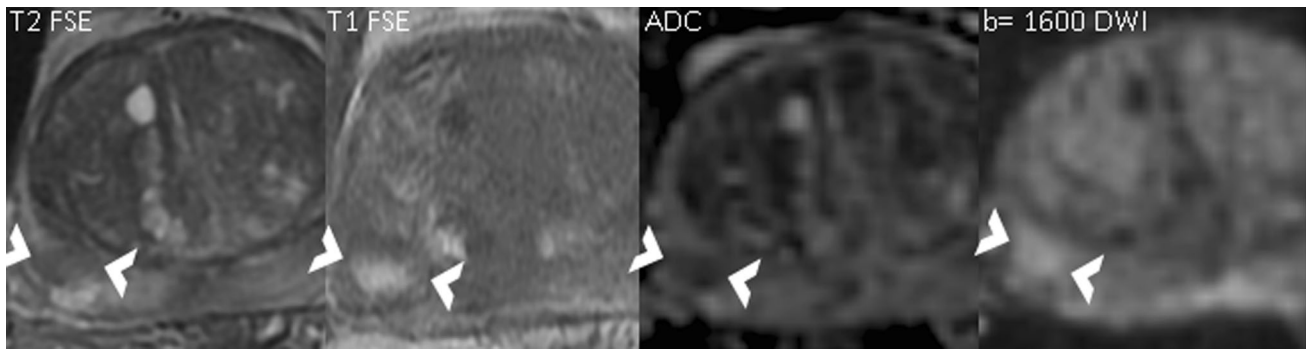


Fig. 4. An area of T2 hypointensity, ADC hypointensity, and mild DWI hyperintensity in the right peripheral zone would correspond to a DWI component score of PI-RADS 4. However, the hyperintense signal on the T1-weighted images

denotes underlying hemorrhage which makes evaluation unreliable. On prostatectomy, there was no malignancy in this portion of the prostate.

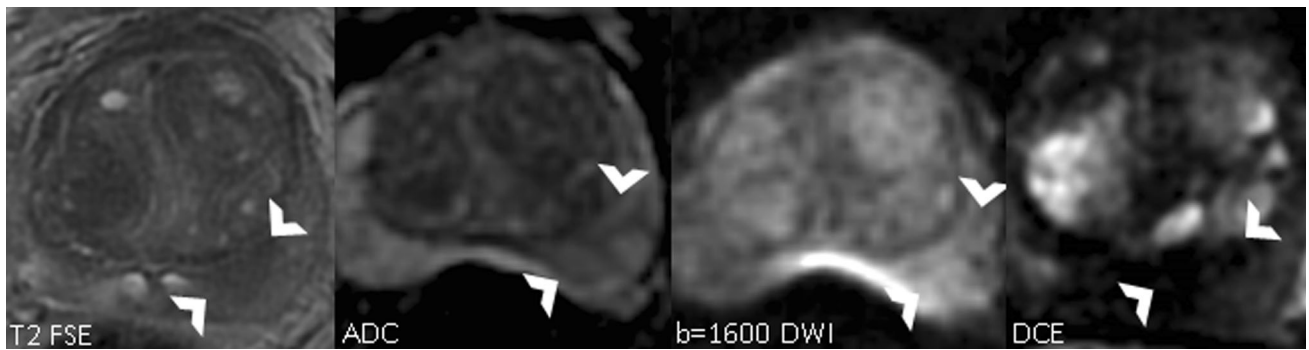


Fig. 5. The left peripheral zone lesion which is moderately T2 hypointense is mildly hypointense on ADC and isointense on DWI images, consistent with a DWI component score of PI-RADS 3. No enhancement is seen on the subtraction

images, making this consistent with an overall assessment score of PI-RADS 3. This lesion was targeted with an MR/US fusion biopsy and was benign.

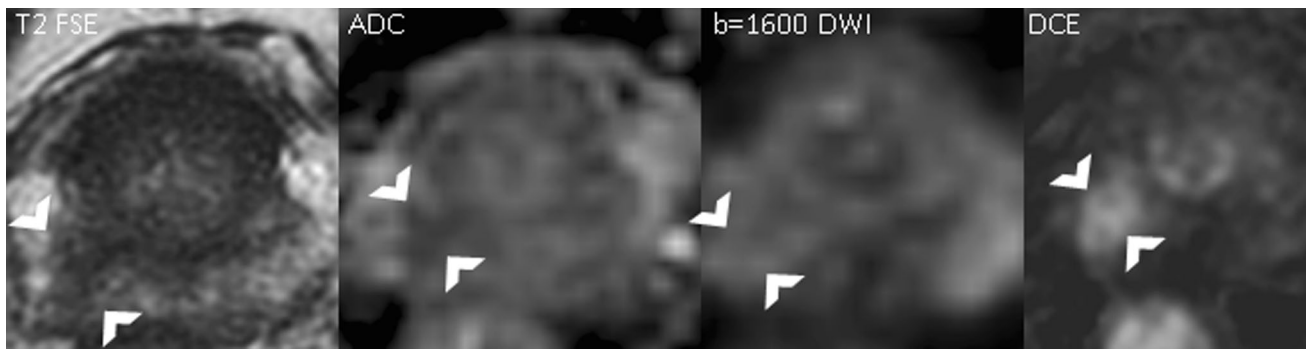


Fig. 6. A small, nodular focus within the right peripheral zone is moderately hypointense on T2-weighted images. On diffusion images alone, this is mildly hypointense on ADC and isointense on DWI, consistent with a DWI component score of PI-RADS 3. However, since there is enhancement on sub-

traction images, the overall assessment is upgraded to PI-RADS 4. On prostatectomy 3 months after this MRI, the patient had Gleason 7 prostate cancer with extraprostatic extension in the right posterior prostate.

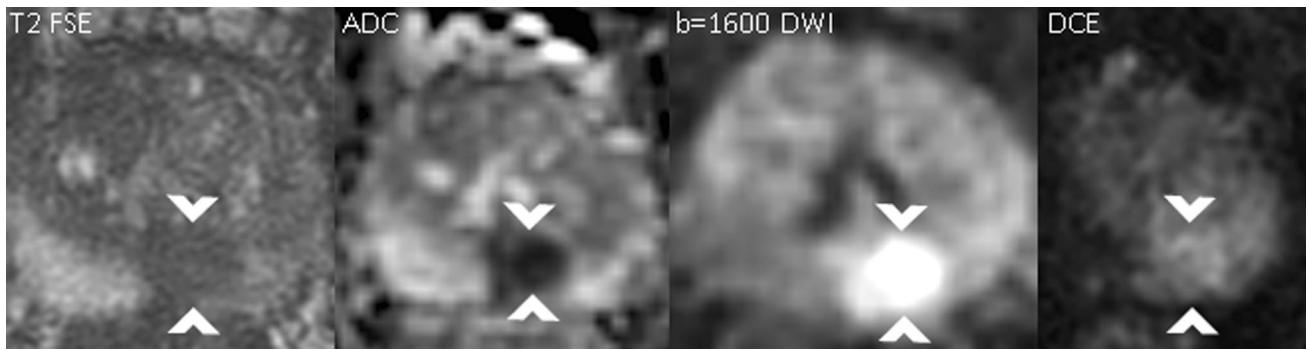


Fig. 7. A round mass in the left peripheral zone is moderately hypointense on T2-weighted images. This is markedly hyperintense on DWI and markedly hypointense on ADC where it measures 0.9 cm, consistent with a PI-RADS 4 le-

sion. Of note, there is only minimal enhancement on the subtraction images. In lesions with markedly restricted diffusion, DCE plays no role in PI-RADS scoring. This was a Gleason 9 cancer on non-targeted biopsy.

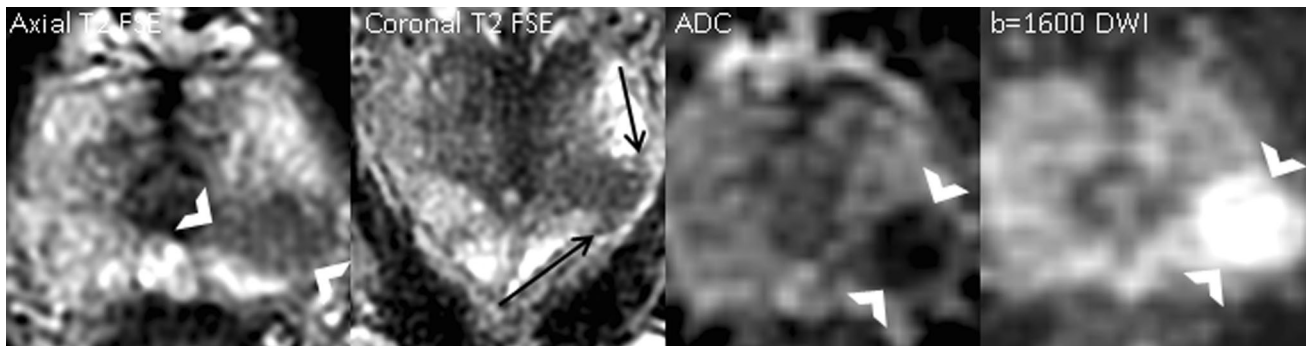


Fig. 8. A left peripheral zone lesion is moderately hypointense on T2-weighted images, markedly hyperintense on DWI, and markedly hypointense on ADC where it measures 1.3 cm. By size and restriction, this would have a DWI component score of PI-RADS 4. However, since there is extra-

capsular extension as denoted by the black arrows on the coronal T2 FSE images, this receives an overall assessment score of PI-RADS 5. On prostatectomy 2 weeks after this MRI, this patient had Gleason 7 prostate cancer in the left posterior quadrant with extracapsular extension.

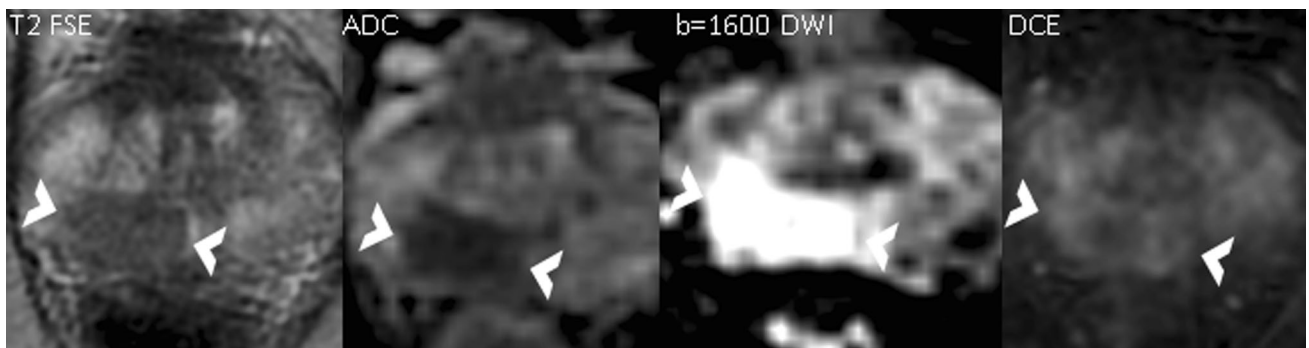


Fig. 9. The right peripheral zone lesion is moderately hypointense on T2 images, markedly hyperintense on DWI, and markedly hypointense on ADC where it measures 1.6 cm,

consistent with a PI-RADS 5 lesion. On prostatectomy, this was a Gleason 7 cancer with invasion of the seminal vesicles.

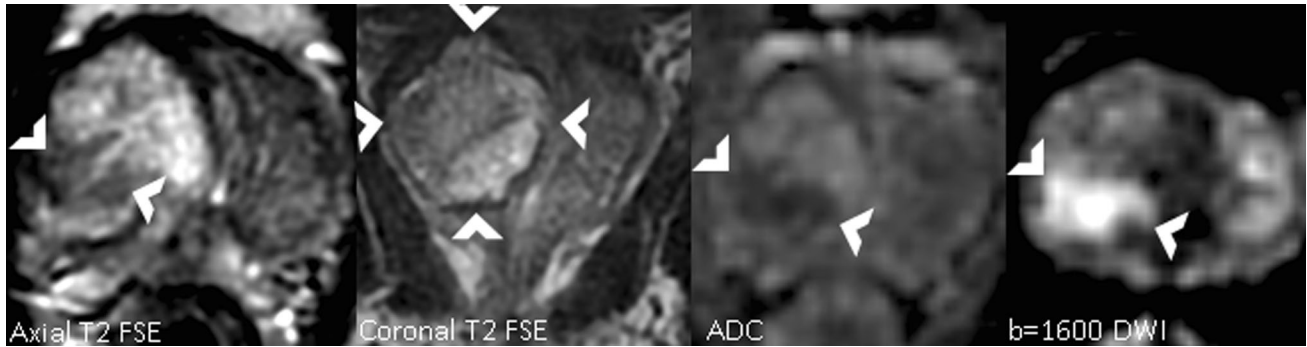


Fig. 10. The right transition zone ill-defined lesion on initial evaluation of axial T2 images is heterogeneous with obscured margins which would be consistent with a T2 component score of PI-RADS 3. This would be upgraded to an overall assessment score of PI-RADS 4 due to the marked hyperin-

tensity on DWI and marked hypointensity on ADC measuring ≥ 1.5 cm. However, on the coronal images, this ill-defined, heterogeneous hypointensity is located within a circumscribed BPH nodule, making it PI-RADS 2. This lesion was biopsied under MR/US fusion guidance and was benign.

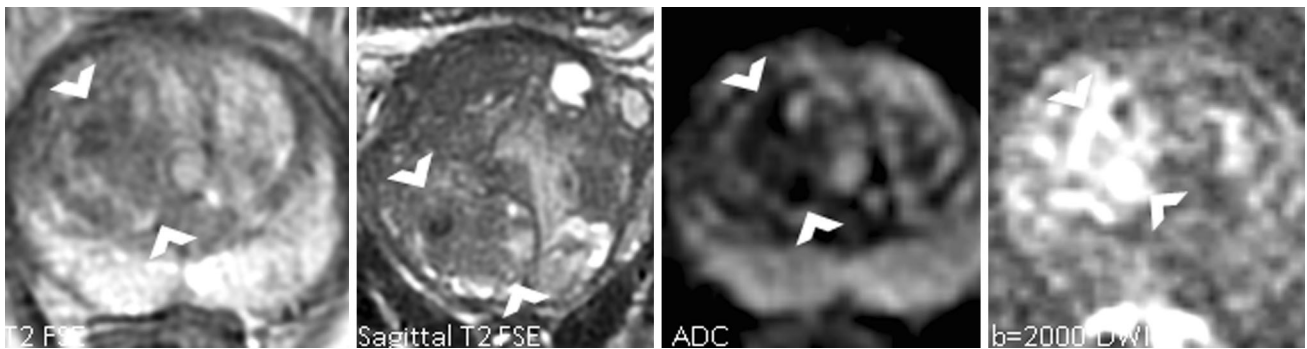


Fig. 11. The right transition zone focus is heterogeneous with obscured margins, denoting a T2 component score of PI-RADS 3. The lesion is markedly hyperintense on DWI images and markedly hypointense on ADC where it measures

< 1.5 cm, consistent with an overall assessment score which remains PI-RADS 3. This lesion was targeted with an MR/US fusion biopsy and was benign.

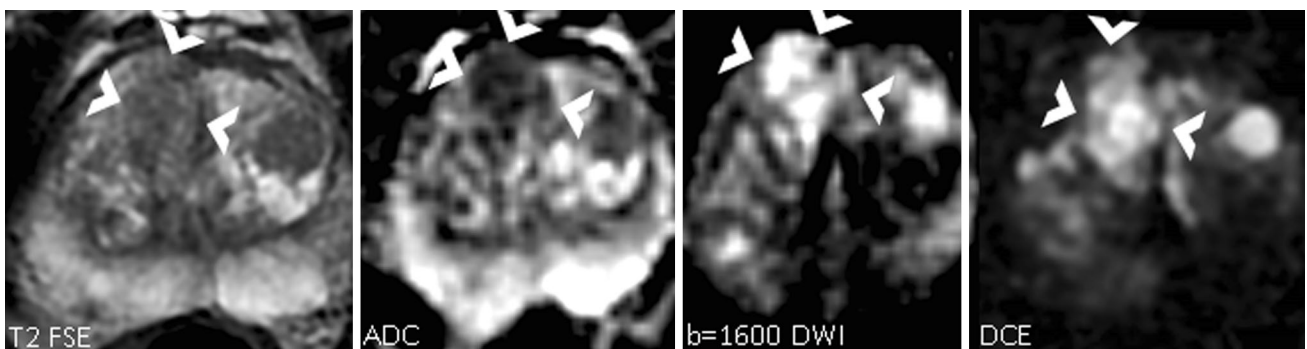


Fig. 12. This right transition zone lesion is heterogeneous with obscured margins on T2-weighted images and receives a T2 component score of PI-RADS 3. However, there is marked DWI hyperintensity and ADC hypointensity which measures ≥ 1.5 cm within the lesion, giving this an overall assessment score of PI-RADS 4. The DCE image shows enhancement in

the region of heterogeneity on the T2-weighted images, corroborating the presence of a lesion. However, the enhancement does not contribute to the PI-RADS score in the transition zone. This lesion was targeted with an MR/US fusion biopsy and was benign.

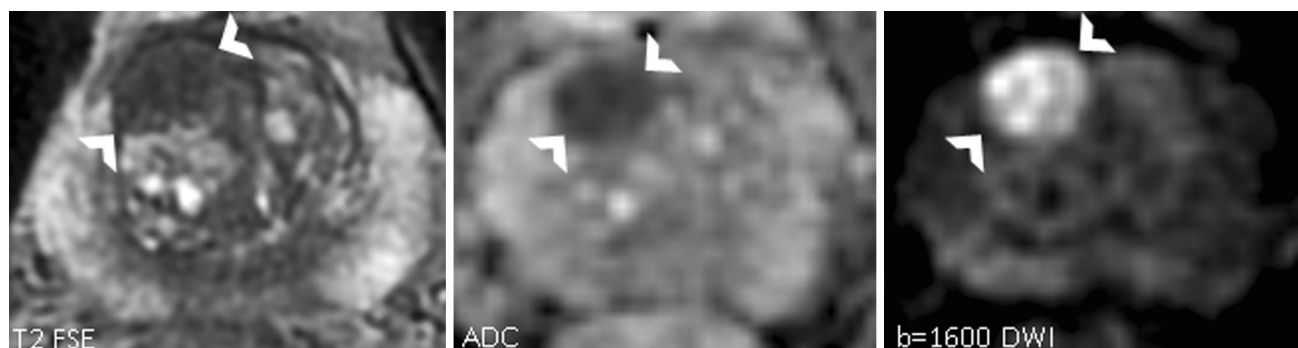


Fig. 13. This homogeneously moderately hypointense T2 signal right anterior transition zone 1.4 cm lesion is lenticular and has a non-circumscribed posterior border, most consistent with a PI-RADS 4 lesion. The restricted diffusion cor-

roborates the finding that this is likely to be clinically significant prostate adenocarcinoma. On prostatectomy, this was a Gleason 7 cancer without extraprostatic extension.

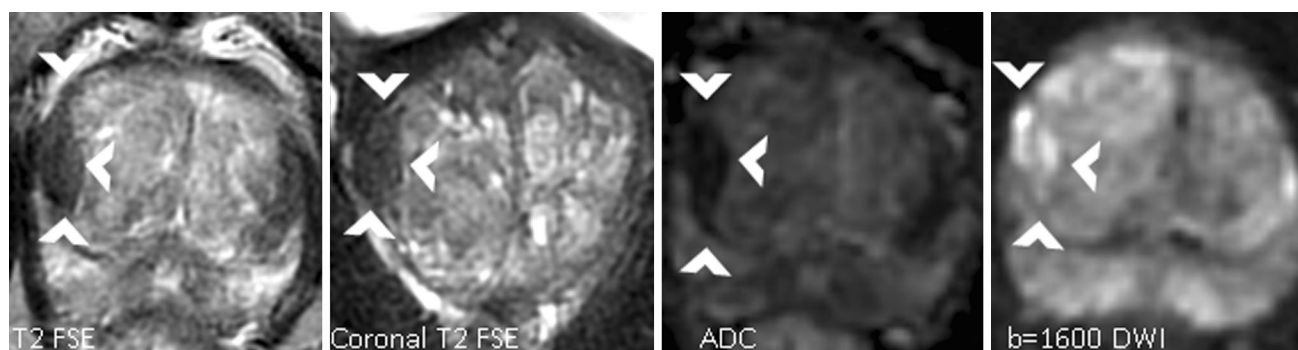


Fig. 14. A right transition zone lenticular area of homogeneously low T2 signal measures 2.3 cm, consistent with an overall assessment score of PI-RADS 5. The marked DWI hyperintensity and ADC hypointensity corroborate that this is

highly likely to be clinically significant prostate adenocarcinoma. This lesion was targeted with an MR/US fusion biopsy and found to be a Gleason 7 prostate cancer.

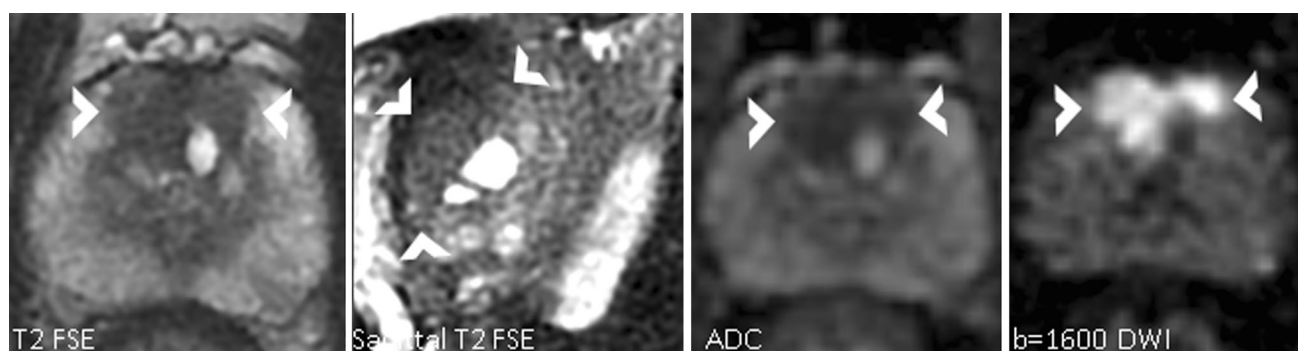


Fig. 15. A homogeneously low T2 signal lesion in the anterior transition zone is non-circumscribed and measures 2.2 cm, extending into the fibromuscular stroma. On T2 characteristics alone, this would be considered a PI-RADS 5 lesion. The homogeneously low T2 signal, infiltrative appearance, and marked restricted diffusion all corroborate

the finding that this is highly likely to be clinically significant prostate adenocarcinoma. This lesion was targeted with an MR/US fusion biopsy and found to be a Gleason 6 prostate cancer. Even though this was Gleason 6 prostate adenocarcinoma, given its large size and infiltrative appearance, this is clinically significant.

for each PI-RADS category (Figs. 4, 5, 6, 7, 8, 9, 10, 11, 12, 13, 14, 15).

Compliance with ethical standards

Conflict of interest None of the authors reported conflicts of interest for this paper.

Ethical approval All procedures performed in studies involving human participants were in accordance with the ethical standards of the institutional and/or national research committee and with the 1964 Helsinki declaration and its later amendments or comparable ethical standards.

Informed consent This is a review article/pictorial essay, and informed consent was not needed since only images which were already obtained were used.

References

1. PI-RADS™ Prostate Imaging-Reporting and Data System Version 2. (2015). [http://www.acr.org/~media/ACR/Documents/PDF/Quality Safety/Resources/PIRADS/PIRADS%20V2.pdf](http://www.acr.org/~media/ACR/Documents/PDF/Quality%20Safety/Resources/PIRADS/PIRADS%20V2.pdf). Accessed 11/19/2015
2. Vargas HA, Hotker AM, Goldman DA, et al. (2015) Updated prostate imaging reporting and data system (PIRADS v2) recommendations for the detection of clinically significant prostate cancer using multiparametric MRI: critical evaluation using whole-mount pathology as standard of reference. *Eur Radiol.* doi:10.1007/s00330-015-4015-6
3. Zhang ZX, Yang J, Zhang CZ, et al. (2014) The value of magnetic resonance imaging in the detection of prostate cancer in patients with previous negative biopsies and elevated prostate-specific antigen levels: a meta-analysis. *Acad Radiol* 21(5):578–589. doi:10.1016/j.acra.2014.01.004
4. Moore CM, Robertson NL, Arsanious N, et al. (2013) Image-guided prostate biopsy using magnetic resonance imaging-derived targets: a systematic review. *Eur Urol* 63(1):125–140. doi:10.1016/j.eururo.2012.06.004
5. Abdi H, Zargar H, Goldenberg SL, et al. (2015) Multiparametric magnetic resonance imaging-targeted biopsy for the detection of prostate cancer in patients with prior negative biopsy results. *Urol Oncol* 33(4):e161–e167. doi:10.1016/j.urolonc.2015.01.004
6. Abdi H, Pourmalek F, Zargar H, et al. (2015) Multiparametric magnetic resonance imaging enhances detection of significant tumor in patients on active surveillance for prostate cancer. *Urology* 85(2):423–428. doi:10.1016/j.urology.2014.09.060
7. Puech P, Rouviere O, Renard-Penna R, et al. (2013) Prostate cancer diagnosis: multiparametric MR-targeted biopsy with cognitive and transrectal US-MR fusion guidance versus systematic biopsy—prospective multicenter study. *Radiology* 268(2):461–469. doi:10.1148/radiol.13121501
8. Tamada T, Kanomata N, Sone T, et al. (2014) High b value (2,000 s/mm²) diffusion-weighted magnetic resonance imaging in prostate cancer at 3 Tesla: comparison with 1000 s/mm² for tumor conspicuity and discrimination of aggressiveness. *PLoS One* 9(5):e96619. doi:10.1371/journal.pone.0096619